Anti-inflammatory mechanism of berberine on lipopolysaccharide-induced IEC-18 models based on comparative transcriptomics

XIAOFAN XU, LE ZHANG, YA ZHAO, BAOYANG XU, WENXIA QIN,
YIQIN YAN, BOQI YIN, CHUYU XI and LIBAO MA

Department of Animal Nutrition and Feed Science, College of Animal Science and Technology,
Huazhong Agricultural University, Wuhan, Hubei 430070, P.R. China

Abstract. Intestinal surface epithelial cells (IECs) have long been considered as an effective barrier for maintaining water and electrolyte balance, and are involved in the mechanism of nutrient absorption. When intestinal inflammation occurs, it is often accompanied by IEC malfunction. Berberine (BBR) is an isoquinoline alkaloid found in numerous types of medicinal plants, which has been clinically used in China to treat symptoms of gastrointestinal pathogenic bacterial infection, especially bacteria-induced diarrhea and inflammation. In the present study, IEC-18 rat intestinal epithelial cells were treated with lipopolysaccharide (LPS) to establish an *in vitro* model of epithelial cell inflammation, and the cells were subsequently treated with BBR in order to elucidate the anti-inflammatory mechanism. Transcriptome data were then searched to find the differentially expressed genes (DEGs) compared between two of the treatment groups (namely, the LPS and LPS+BBR groups), and DEGs were analyzed using Gene Ontology, Kyoto Encyclopedia of Genes and Genomes, Weighted Gene Correlation Network Analysis and Interactive Pathways Explorer to identify the functions and pathways enriched with DEGs. Finally, reverse transcription-quantitative PCR was used to verify the transcriptome data. These experiments revealed that, comparing between the LPS and LPS+BBR groups, the functions and pathways enriched in DEGs were 'DNA replication', 'cell cycle', 'apoptosis', 'leukocyte migration' and the 'NF-κB and AP-1 pathways'. The results revealed that BBR is able to restrict DNA replication, inhibit the cell cycle and promote apoptosis. It can also inhibit the classic inflammatory pathways, such as those mediated by NF-κB and AP-1, and the expression of various chemokines to prevent the migration of leukocytes. According to transcriptomic data, BBR can exert its anti-inflammatory effects by regulating a variety of cellular physiological activities, including cell cycle, apoptosis, inflammatory pathways and leukocyte migration.

Introduction

Inflammation is the body's response to harmful stimuli and it is usually beneficial to our health. It is triggered as an automatic defense response, but occasionally it can also be harmful to our bodies, through attacking bodily tissues. Severe inflammation results in a series of diseases, including cancer (1), diabetes (2), cardiovascular diseases (3) and metabolic diseases (4). Recent evidence has suggested that the intestinal epithelium contributes to the development and perpetuation of inflammation in different types of inflammatory bowel diseases (IBDs), including ulcerative colitis (UC) and Crohn's disease (CD) (5). While both UC and CD share an exaggerated immune response and some common symptoms, such as neutrophil aggregation and plasma cell invasion, as their pathological markers, there are differences related to their location within the gastrointestinal tract (6). UC is a chronic non-specific inflammation of the colon. In severe cases, the patient will develop ulcers. The lesions are mainly located in the colonic mucosa and submucosa, and are distributed continuously (7). CD is a chronic granulomatous inflammation that affects all parts of the gastrointestinal tract, especially the ileum, and presents a segmental distribution (8). In addition to functioning as a barrier, intestinal epithelial cells (IECs) act both as sensors for pathogen- and damage-associated molecular patterns and as regulators of immune cells (9,10). Therefore, in the present study IEC-18 cells, which are a rat ileum epithelial cell line, were used to investigate the effect of berberine (BBR) in IBD, especially in CD.

Lipopolysaccharide (LPS), an endotoxin obtained from Gram-negative bacteria, is able to exert its physiological effects by interacting with toll-like receptor 4 (TLR4), a

Correspondence to: Professor Libao Ma, Department of Animal Nutrition and Feed Science, College of Animal Science and Technology, Huazhong Agricultural University, 1 Shizishan Street, Hongshan, Wuhan, Hubei 430070, P.R. China
E-mail: malibao@mail.hzau.edu.cn

member of the TLR family, on the cell-membrane surface of host cells (11). The TLR family is associated with the expression of inflammatory cytokines, and has an important role in natural immunity (12). LPS has been widely used as a model of inflammation to study the anti-inflammatory influence of drugs or other bioactive compounds. For example, LPS was used as the inflammatory model to study the mechanism underlying how the flavonoid luteolin may prevent LPS-induced NF-κB signaling and gene expression (13).

BBR is an isoquinoline alkaloid found as the major alkaloid in numerous types of medicinal plants, including the families Papaveraceae, Berberidaceae, Fumariaceae, Menispermaceae, Ranunculaceae, Rutaceae and Annonaceae (14). BBR has been used as an over-the-counter drug in the clinical treatment of diarrhea, but modern pharmacological studies have demonstrated that BBR has significant antiarrhythmic, antiplatelet and anti-inflammatory effects, has the ability to reduce cholesterol levels and vascular smooth muscle proliferation, and can improve insulin resistance (15). The primary anti-inflammatory pharmacological action of BBR is to inhibit the production and activity of inflammatory cytokines (16). Since BBR has been widely used as an anti-inflammatory drug, it was found to be a causative agent in inactivating the NLRP3 inflammasome in monosodium urate crystal-induced inflammation (17). Additionally, BBR was revealed to inhibit the basal and 12-O-tetradecanoylphorbol-13-acetate (TPA)-mediated levels of prostaglandin E2 and cyclooxygenase-2 (COX-2) expression by inhibiting the binding of AP-1 (18). BBR also upregulated activating transcription factor 3 (ATF-3) expression in murine macrophages, subsequently reducing proinflammatory cytokine production via TLR signaling (19). BBR potently suppressed the inflammatory response in macrophages by inhibiting NF-κB signaling via sirtuin-1-dependent mechanisms (20). Administration of BBR can notably ameliorate disease severity and restore the mucosal barrier homeostasis of patients with UC (21), and upregulate P-glycoprotein via activation of nuclear factor erythroid 2-related factor 2-dependent mechanisms to improve symptoms in patients with UC (22). BBR also inhibits inflammatory responses as well as T helper cell (Th)1/Th7 differentiation to ameliorate 2,4,6-Trinitrobenzenesulfonic acid solution (TNBS)-induced IBD (23). However, the transcriptome analysis has rarely been applied to interpret the pharmacological action of BBR. To the best of our knowledge, the present study is the first attempt that has been made at applying transcriptomics to elucidate the anti-inflammatory mechanisms underlying the effects of BBR on an LPS-induced *in vivo* inflammation model.

The efficacy of BBR in different disease states has led to an increased interest in its pharmacological activities. However, the number of unrelated molecules that are targeted by BBR makes it a complicated challenge to unravel its mechanism of action. The mechanism underlying its anti-inflammatory activity remains unclear, in spite of the significant amount of relevant data that are available.

In the present study, high-throughput RNA sequencing, as well as functional enrichment of Gene Ontology (GO) terms, Kyoto Encyclopedia of Genes and Genomes (KEGG) pathway analysis and Weighted Gene Correlation Network Analysis (WGCNA), were applied to analyze differentially expressed genes (DEGs) between LPS-induced and BBR-treated groups. The objective of the present study was to reveal the anti-inflammatory mechanism of BBR in an LPS-induced IEC-18 inflammatory model at the transcriptome level. The results obtained herein may help to further unveil the mechanisms of BBR's anti-inflammatory action.

Materials and methods

Cells and drugs. Rat IECs (IEC-18 cell line) were purchased from Hunan Fenghui Biotechnology Co., Ltd., and BBR (PubChem CID: 2353) was purchased from Merck KGaA. DMSO was also purchased from Merck KGaA, and Gibco® DMEM was purchased from Thermo Fisher Scientific, Inc.

Sample treatment and collection. A total of four treatment groups were devised for the experiments in the present study (the control group, the LPS group, the LPS+BBR group and the LPS+DMSO group). Cells in the control group were cultured in normal culture medium for 12 h, and then total RNA was collected from the cells using TRIzol® reagent (Invitrogen; Thermo Fisher Scientific, Inc.). Cells in the LPS group were cultured in culture medium with LPS (10 μg/ml) (Sigma-Aldrich; Merck KGaA) for 12 h prior to collection of the total RNA from the cells. Cells in the LPS+BBR group were cultured in culture medium with LPS (10 μg/ml) for 12 h, and subsequently cultured in culture medium with BBR (100 μM) for a further 24 h, after which the total RNA was collected from the cells. Finally, cells in the LPS+DMSO group were cultured in culture medium with LPS (10 μg/ml) for 12 h, and subsequently cultured in culture medium with DMSO (0.2%) for a further 24 h, after which the total RNA was collected from the cells. BBR was dissolved in DMSO (0.2%). For all of the experiments, IEC-18 cells (1x10^6) were cultured in DMEM containing 10% fetal bovine serum (FBS) (Invitrogen; Thermo Fisher Scientific, Inc.), 1% penicillin/streptomycin and 0.1 μg/ml insulin at 37°C under an atmosphere of 5% CO_2. Total RNA was extracted from the cells using TRIzol reagent, according to the manufacturer's instructions, and genomic DNA was removed using DNase I (Takara Biotechnology Co., Ltd.). Finally, the RNA quality was determined using an Agilent 2100 Bioanalyzer (Agilent Technologies, Inc.) and quantified using a NanoDrop 2000 instrument (NanoDrop Technologies; Thermo Fisher Scientific, Inc.), according to the manufacturer's instructions.

MTT cell viability assay. The MTT assay was performed following a previous experiment by Mosmann (21). Cells were cultured in 96-well plates at a density of 1x10^4 cells per well. The four groups were treated for 0, 4, 8, 12, 16, 20 and 24 h. After incubation, 10 μl MTT (5 mg/ml in H_2O) was added to each well and incubation continued for a further 4 h at 37°C. The culture media containing MTT were aspirated and 150 μl DMSO was then added into each well to dissolve the formazan crystals, and subsequently the absorbance of each well was recorded at 570 nm using a BioTek ELISA microplate reader (BioTek Instruments, Inc.). Cell viability was estimated by dividing the absorbance of treated cells in each well to the mean absorbance of the control. The values were calculated from three independent experiments. Data are presented as the mean ± SD (n=3).

Library preparation and Illumina HiSeq 4000 sequencing. The RNA-seq transcriptome library was prepared following

the TruSeq™ RNA sample preparation kit from Illumina, Inc., using 5 µg total RNA. Libraries were selected for cDNA target fragments of 200-300 bp on 2% low range ultra agarose, followed by PCR amplification using Phusion DNA polymerase (New England BioLabs, Inc.) for 15 PCR cycles (forward primer, 5'-AGATCGGAAGAGCACACG TC-3'; reverse primer, 5'AGATCGGAAGAGCGTCGTGT-3') under the following thermocycling conditions: 50°C for 2 min, 95°C for 10 min, 95°C for 30 sec and 60°C for 30 sec (24). After quantification using a TBS-380 Mini-Fluorometer, the paired-end RNA-seq sequencing library was sequenced with the Illumina HiSeq 4000 System (2x150 bp read length).

Data analysis. The expression of each transcript was calculated according to the fragments per kilobase of exon per million mapped reads (FPKM) method (24). RNA-seq by expectation-maximization (version 2.2.0; deweylab.biostat.wisc.edu/rsem/) was used to quantify the abundance of the genes. DEGs were identified through pairwise comparisons using EdgeR (Empirical analysis of Digital Gene Expression in R) (version 4.0; bioconductor. org/packages/release/bioc/html/edgeR.html). Genes having an abundance with a fold-change ≥2 and P<0.05 were considered to be regulated differently in the four comparison groups (control vs. LPS; LPS vs. LPS+BBR; LPS vs. LPS+DMSO; and LPS+BBR vs. LPS+DMSO). To further investigate the biological processes associated with DEGs, GO analysis (25,26) was performed by running queries for each DEG against the GO database, which provided information on the relevant 'molecular functions', 'cellular components' and 'biological processes'. KEGG functional-enrichment analysis (27) was subsequently performed to identify the DEGs that were significantly enriched in anti-inflammatory pathways (P≤0.05) compared with the whole-transcriptome background. Principal component analysis (PCA) and hierarchical clustering analysis (HCA) were also performed to assess the similarities and differences in transcriptome profiles using the online software MetaboAnalyst 4.0 (metaboanalyst.ca/).

WGCNA analysis. WGCNA was performed on normalized counts of RNA-Seq data. An adjacency matrix was built with a soft thresholding value of 7, based on the recommendation of the WGCNA tutorial (horvath.genetics.ucla. edu/html/CoexpressionNetwork/Rpackages/WGCNA/index. html). A gene cluster dendrogram was constructed with a height cutoff of 0.25.

Interactive pathways explorer analysis. By using iPath3.0 (pathways.embl.de) to make a visual analysis of metabolic pathways, the metabolic pathway information of the whole biological system was viewed. The nodes represent different compounds; boundaries represent different enzymatic reactions.

Reverse transcription-quantitative PCR (RT-qPCR). RT-qPCR analysis was performed to validate the expression of crucial DEGs. According to the manufacturer's instructions, total RNA was extracted with TRIzol reagent (Invitrogen; Thermo Fisher Scientific, Inc.) from different groups, including control group, LPS-stimulated inflammatory models, and the BBR

and DMSO groups. Total RNA (2 µg) was reverse-transcribed (25°C for 10 min, 50°C for 45 min and 85°C for 5 min) into single-stranded cDNA using HiScript Reverse Transcriptase (Vazyme Biotech Co., Ltd.). RT-qPCR was subsequently performed with the following thermocycling conditions: 50°C for 2 min, 95°C for 10 min, 95°C for 30 sec and 60°C for 30 sec. All reactions were processed in triplicate for 40 cycles using a QuantStudio 6 Flex Real-Time PCR System (Applied Biosystems; Thermo Fisher Scientific, Inc.) and the fluorophore was SYBR Green I (Thermo Fisher Scientific, Inc.). The relative expression was calculated according to the $2^{-\Delta\Delta Cq}$ method (28). The relevant oligonucleotide sequences of primers are presented in Table SI. β-actin was used as a reference gene in RT-qPCR.

Statistical analysis. Results are presented as the mean ± SEM. RNA-seq experimental data were analyzed by one-way ANOVA followed by the Duncan's multiple comparison post hoc test using GraphPad 8.0 software (GraphPad Software, Inc.). P<0.05 was considered to indicate a statistically significant difference.

Results

Cell viability assay. In the present trial, an LPS-induced inflammatory cell model was established and then treated with BBR. The anti-inflammatory effect of BBR was performed by measuring the cell viability of IEC-18 cells using an MTT assay. The cell viability of four groups is presented in Fig. 1. The results showed that BBR can increase the cell viability of IEC-18 cells, compared with the LPS and LPS+DMSO groups.

Gene identification. In the present study, an average of 52,040,757 raw reads from the control, LPS, LPS+BBR and LPS+DMSO group samples were obtained, and the average number of clean reads was 51,420,009. All the downstream analyses were based on high-quality clean data and the error rates were all <0.025%. The clean reads were mapped to the mouse reference genome sequence, and 95.56-95.91% of the clean reads in the libraries were mapped to the rat reference genome (Table I).

Comparative transcriptomic analysis. To investigate the genes of interest associated with anti-inflammation and their expression patterns, the coding genes among the different groups that were expressed specifically in the cells were compared and characterized. In total, 11,732, 11,923, 11,829 and 11,953 genes were found to have expression levels >0.1 FPKM in the control, LPS, LPS+BBR and LPS+DMSO groups, respectively. The expression of ~11,258 of the genes (90.4% of the total number of coding genes) was shared by the four groups. On the other hand, there were 117, 89, 114 and 118 genes expressed uniquely in the control, LPS, LPS+BBR and LPS+DMSO groups, respectively (Fig. 2A).

PCA was used to display the associations among the transcriptomes representing the largest variance in the datasets. As expected, replicates for each group were closer to each other than they were to the other groups. Principal component (PC)1, which accounted for 35.87% of the variance, separated the control group from the other groups. PC2, which accounted
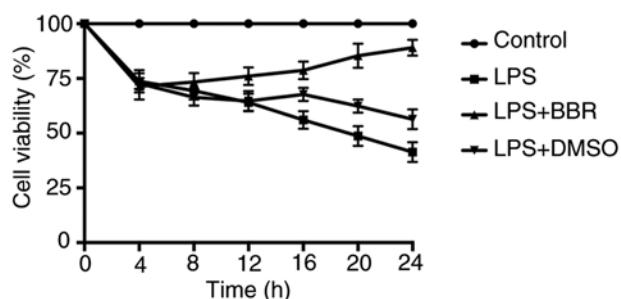
Figure 1. Cell viability assay. Cell viability was measured by an MTT assay, IEC-18 cells were divided into four groups, and these groups were treated for 0, 4, 8, 12, 16, 20 and 24 h. The cell viability was estimated by dividing the absorbance of treated cells in each group to the mean absorbance of the control. The values were calculated from three independent experiments. Data are presented as the mean ± SD (n=3). LPS, lipopolysaccharide; BBR, berberine.

for 13.6% of the total variance, separated the BBR group from all other groups (Fig. 2B). Of note, the transcriptomes of the BBR group were found to be markedly different from those of the LPS group, although they were close to those of the control group; by contrast, the DMSO group was similar to the LPS group.

HCA was performed to oversee the transcriptomic changes within different samples from the control, LPS, LPS+BBR and LPS+DMSO groups (Fig. 3A). The heatmap presents the relative abundance of the gene expression levels, where deep red represents a higher intensity and deep blue represents a lower intensity. Samples are displayed as columns, and different colors were used to indicate the classification of the different subtypes. Cell samples from the control and LPS groups, as well as the LPS and LPS+BBR groups, displayed different color distributions. Different repetitions from the same group exhibited similar transcriptome distributions, and these were first aggregated into a cluster. With an increase in Euclidean distance, the LPS+DMSO and LPS samples were aggregated into a cluster, and these differed from the BBR and control samples, suggesting that significant changes had occurred in the transcriptome following treatment with BBR.

In addition, the scatter diagram shown in Fig. 3B identifies the DEGs with different colors, in which red signifies genes that were upregulated, and green indicates those that were downregulated. In pairwise comparisons between the control and LPS samples, a total of 1,901 genes were found to be differentially expressed, of which 1,289 genes were upregulated and 612 were downregulated in the LPS group. In pairwise comparisons between the LPS and LPS+BBR samples, a total of 1,875 genes were differentially expressed, of which 687 genes were upregulated and 1,188 were downregulated in the LPS+BBR group (Fig. 3B). It is noteworthy that the DEGs between the control and LPS groups were very similar to those between the LPS and LPS+BBR groups, although they exhibited the opposite regulatory effects. Therefore, one may speculate that BBR could be responsible for the occurrence of biochemical events in different samples following treatment.

GO and KEGG pathway analyses. GO analysis not only provides reliable gene product descriptions from various databases, but it also offers a set of dynamic, controlled and structured terminologies to describe gene functions and products in an organism. According to GO functions, all DEGs are routinely classified into three categories: 'Biological process', 'cellular component' and 'molecular function'. In the present study, a total of 59 terms were found to be enriched in GO terms (LPS group vs. the LPS+BBR group), among which 27 were for 'biological process', 17 were for 'cellular component', and 15 were for 'molecular function' (Table SII). Concerning the 'biological process' category, 77.68% genes were annotated into 'cellular process' (GO:0009987), 56.82% genes were involved in 'biological regulation' (GO:0065007), and 54.16% genes were involved in 'metabolic process' (GO:0008152) (Fig. 4). In terms of the 'cellular component' category, 75.27% of the genes were located in 'cell part' (GO:0044464), and 42.82% were in 'organelle part' (GO:0044422) (Fig. 4). Finally, regarding the 'molecular function' category, 69.12% genes were involved in 'binding' (GO:0005488), whereas 34.14% genes were in 'catalytic activity' (GO:0003824) (Fig. 4).

The DEGs (LPS vs. LPS+BBR) in the KEGG pathway database were also mapped, and all the pathways were classified into the following six categories: 'Metabolism' (15.1%), 'Genetic information processing' (5.2%), 'Environmental information processing' (15.5%), 'Cellular processes' (12.4%), 'Organismal systems' (19.4%) and 'Human diseases' (32.4%) (Fig. 5).

To characterize the functional consequences of gene expression changes caused by BBR, GO enrichment analysis of 829 DEGs (LPS group vs. the LPS+BBR group) was performed based on the GO database. Fig. 6A shows the top 20 ranked GO terms of the DEGs. 'DNA replication initiation' showed the highest enrichment degree as it possessed the highest rich factor (0.54), followed by 'kinetochore organization' (rich factor, 0.44). In addition, 'nuclear chromosome segregation' (0.23), 'mitotic cell cycle' (0.15) and 'regulation of chromosome separation' (0.27) were the most abundant functional groups in the majority of the comparisons.

Subsequently, KEGG enrichment analysis was performed. The results showed that most of the annotated genes involved in the top 20 ranked KEGG pathways of DEGs were enriched in 'Steroid biosynthesis' (rich factor, 0.36), 'DNA replication' (0.28), 'TNF signaling pathway' (0.08), and 'Cytokine-cytokine receptor interaction' (0.07) (Fig. 6B).

WGCNA analysis. The total number of 32,883 genes were divided into 25 modules according to similarities in the expression patterns (Fig. 7A). The aim was to focus on the differences between the LPS and the LPS+BBR treatment groups. The results demonstrated that module 'brown' accorded closely with the requirements of the present study, as the correlation coefficient between module 'brown' and the LPS+BBR group was 0.753 (Fig. 7B). To identify the key genes from module 'brown', a gene correlation network was constructed using 1,794 genes in this module. Based on the degree of connectivity, the top 20 genes were regarded as hub genes. The top 5 genes were Vasorin (Vasn), activin receptor type-1B (Acvr1b), NF-kB inhibitor a (Nfkbia), purine nucleoside phosphorylase (Pnp) and disintegrin and metalloprotinease domain-containing protein 17 (Adam17) (Fig. 7C). Vasm was associated with 'cell surface receptor signaling pathway' (GO:0007166), and Acvr1b with 'regulation of transcription from RNA polymerase II

Table I. Reads mapping summary of the four groups.

Sample	Raw reads	Clean reads	Total mapped (%)	Error rate, %	Q20, %	Q30, %	GC content, %
Control 1	46,524,694	46,012,484	43,968,009 (95.56)	0.0239	98.42	95.31	51.44
Control 2	55,153,734	54,522,550	52,161,079 (95.67)	0.0241	98.34	95.11	51.22
Control 3	51,084,072	50,472,388	48,406,455 (95.91)	0.0246	98.16	94.64	51.60
LPS 1	54,040,422	53,383,494	51,070,101 (95.67)	0.0244	98.20	94.78	51.92
LPS 2	53,793,660	53,156,402	50,867,107 (95.69)	0.0242	98.31	95.04	51.87
LPS 3	48,673,560	48,055,566	45,998,851 (95.72)	0.0243	98.23	94.88	51.89
LPS+BBR 1	55,773,654	55,091,394	52,759,191 (95.77)	0.0244	98.22	94.83	52.65
LPS+BBR 2	51,508,862	50,889,204	48,767,843 (95.83)	0.0242	98.31	95.03	52.53
LPS+BBR 3	48,967,886	48,415,432	46,393,264 (95.82)	0.0240	98.36	95.16	52.16
LPS+DMSO 1	47,007,982	46,428,692	44,443,027 (95.72)	0.0241	98.32	95.08	51.97
LPS+DMSO 2	56,177,300	55,495,184	53,114,736 (95.71)	0.0243	98.26	94.92	52.43
LPS+DMSO 3	55,783,230	55,117,324	52,849,178 (95.88)	0.0244	98.22	94.81	52.12

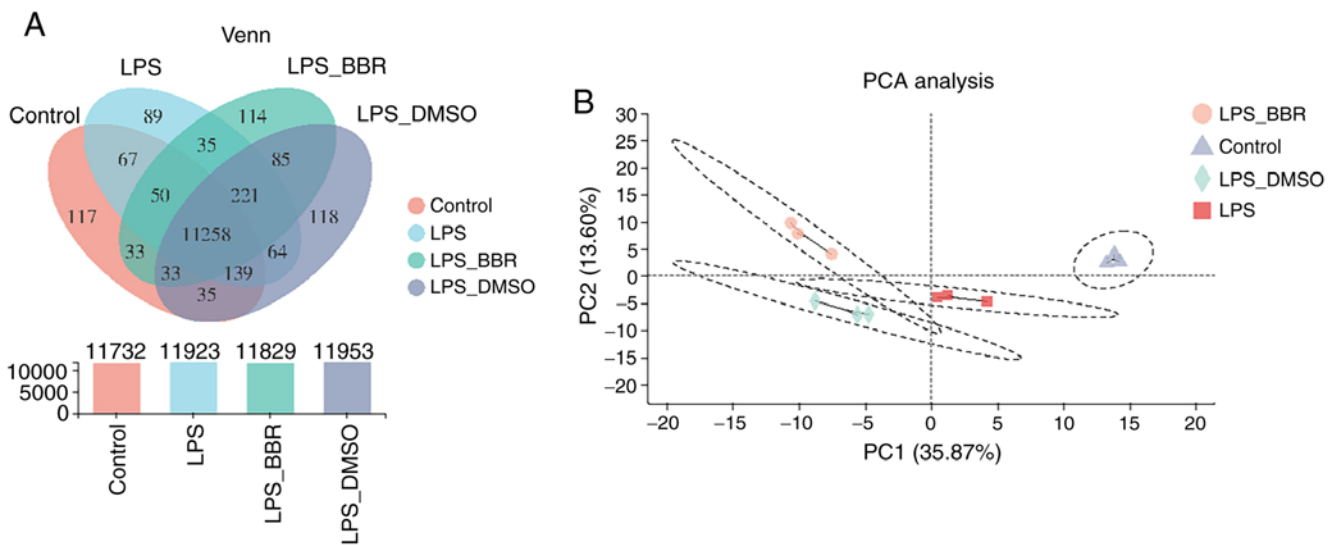LPS, lipopolysaccharide; BBR, berberine; G, guanine; C, cytosine.

Figure 2. Correlation analysis of gene expression. (A) Venn analysis showing the number of co-expression and specific expression genes between samples or between groups. (B) PCA analysis was based on expression level clustering of samples. LPS, lipopolysaccharide; BBR, berberine; PCA, principal component analysis.

promoter' (GO:0045944) and 'positive regulation of activin receptor signaling pathway' (GO:0032927). Nfkbia was associated with 'regulation of NF-κB transcription factor activity' (GO:0032088) and 'Toll-like receptor 4 signaling pathway' (GO:0034142). Pnp was associated with 'regulation of a-b T cell differentiation' (GO:0046638) and 'interleukin-2 secretion' (GO:0070970). Adam17 was associated with 'regulation of protein phosphorylation' (GO:0001934) and 'Notch signaling pathway' (GO:0007219) (Table SIII). Subsequently, KEGG enrichment analysis was performed on the genes involved in module 'brown'. The results revealed that the majority of the annotated genes involved in the top 15 ranked KEGG pathways of module 'brown' were enriched in 'Endocytosis', 'TNF-signaling pathway', 'Chemokine signaling pathway', 'Toll-like receptor signaling pathway' and 'MAPK signaling pathway' (Fig. 8).

Metabolic network analysis. Interactive Pathways Explorer (iPath) was employed to improve the understanding of the global differential biological metabolic response between the LPS and LPS+BBR groups. iPath analysis revealed the presence of 538 DEGs, mainly focused on 'Amino acid metabolism' (Fig. 9A), 'Nucleotide metabolism' (Fig. 9B) and 'Lipid metabolism' (Fig. 9C).

Genes involved in DNA replication and cell cycle. A total of 27 genes associated with the cell cycle were detected with significantly different expression patterns between the LPS and BBR samples (26 genes were downregulated and 1 was upregulated in the BBR group) (Table II). The results of the present study showed that the expression levels of cell division cycle (Cdc) 6, origin recognition complex subunit (Orc) 1, Orc6, minichromosome maintenance complex component
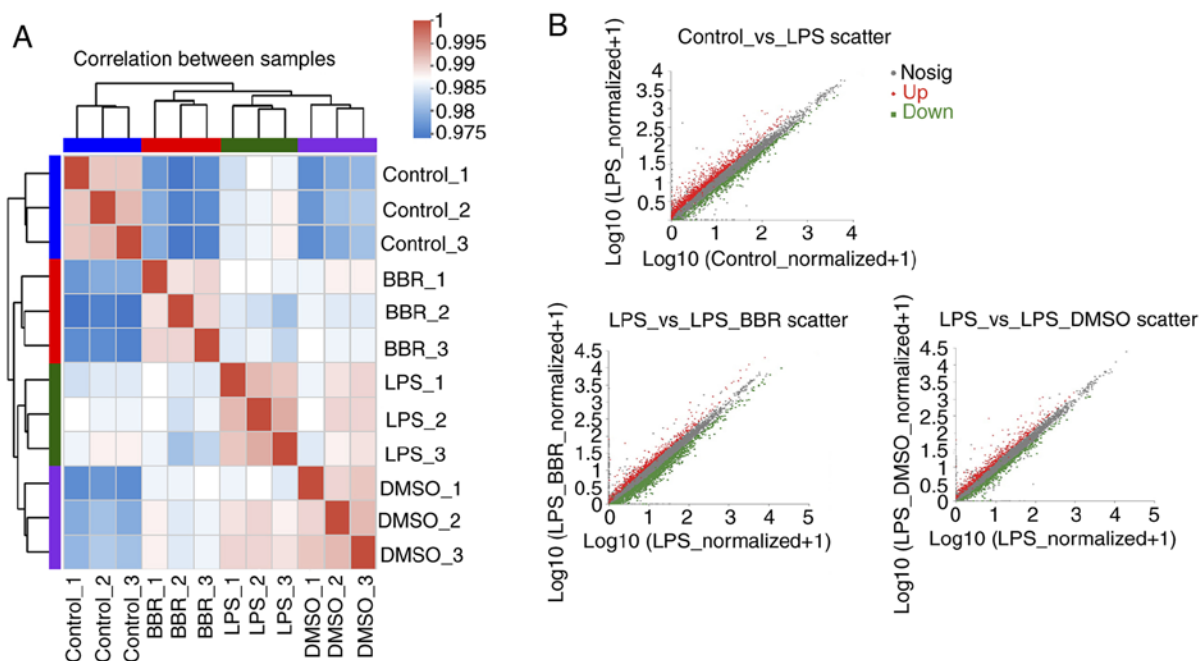
Figure 3. Four groups transcriptome data analysis. (A) Correlation analysis was used to test whether the variation between samples, especially between biological replicates, was consistent with the experimental design. (B) Expression level difference scatter plot reflects the difference in gene expression among groups (red represents upregulation and green represents downregulation). LPS, lipopolysaccharide; BBR, berberine.
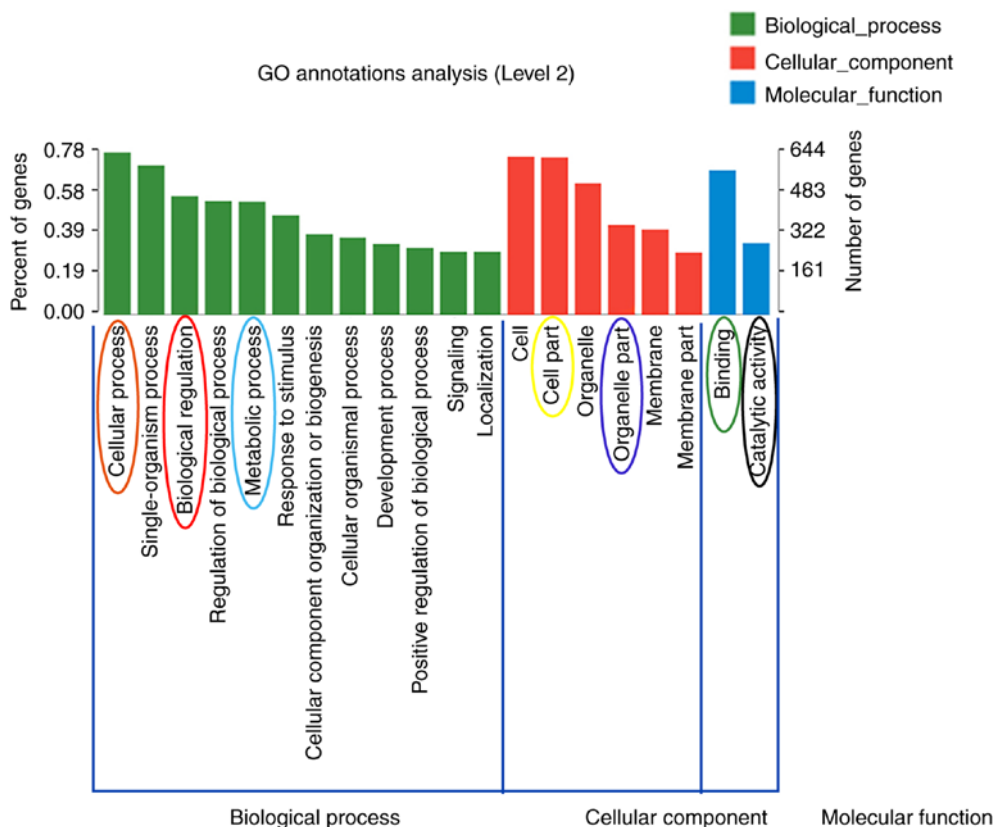

Figure 4. GO annotations analysis. The differentially expressed genes between LPS and LPS+BBR groups were classified into 'biological process', 'cellular component' and 'molecular function' (orange circle, 'cellular process'; red circle, 'biological regulation', blue circle, 'metabolic process'; yellow circle, 'cell part'; purple circle, 'organelle part'; green circle, 'binding'; black circle, 'catalytic activity'). LPS, lipopolysaccharide; BBR, berberine; GO, Gene Ontology.

(Mcm) 3, Mcm4, Mcm5, Mcm6, Mcm7 and Cdc7 were down-regulated in the BBR group compared with the LPS group, which suggested that BBR can restrict DNA replication, thereby inhibiting the cell cycle by regulating these key genes.

Table II. Genes involved in DNA replication and cell cycle.

| LPS_vs._LPS_BBR	Gene ID	Gene name	Gene description
Down	ENSRNOG00000000632	Cdk1	Cyclin-dependent kinase 1
Down	ENSRNOG00000016708	Necab3	N-terminal EF-hand calcium binding protein 3
Down	ENSRNOG00000024043	Orc6	Origin recognition complex subunit 6
Down	ENSRNOG00000054057	AABR07058955.2	-
Down	ENSRNOG00000000521	Cdkn1a	Cyclin-dependent kinase inhibitor 1A
Down	ENSRNOG00000005376	Mad2l1	Mitotic arrest deficient 2 like 1
Down	ENSRNOG00000050071	Cdc45	Cell division cycle 45
Down	ENSRNOG00000014336	Mcm5	Minichromosome maintenance complex component 5
Down	ENSRNOG00000003802	Pttg1	Pituitary tumor-transforming 1
Down	ENSRNOG00000008841	Orc1	Origin recognition complex subunit 1
Down	ENSRNOG00000012543	Mcm3	Minichromosome maintenance complex component 3
Down	ENSRNOG00000007906	Bub1b	BUB1 mitotic checkpoint serine/threonine kinase B
Down	ENSRNOG00000002105	Cdc7	Cell division cycle 7
Down	ENSRNOG00000008055	Ccne2	Cyclin E2
Down	ENSRNOG00000028415	Cdc20	Cell division cycle 20
Down	ENSRNOG00000015423	Ccna2	Cyclin A2
Down	ENSRNOG00000029055	Ttk	Ttk protein kinase
Down	ENSRNOG00000003703	Mcm6	Minichromosome maintenance complex component 6
Down	ENSRNOG00000018815	Plk1	Polo-like kinase 1
Down	ENSRNOG00000053626	AABR07058955.1	-
Down	ENSRNOG00000027787	Cdc6	Cell division cycle 6
Down	ENSRNOG00000001349	Mcm7	Minichromosome maintenance complex component 7
Down	ENSRNOG00000001833	Mcm4	Minichromosome maintenance complex component 4
Down	ENSRNOG00000012835	Espl1	Extra spindle pole bodies like 1 separase
Down	ENSRNOG00000002418	Tgfb2	Transforming growth factor β2
Down	ENSRNOG00000008956	Cdkn2c	Cyclin-dependent kinase inhibitor 2C
UP	ENSRNOG00000061358	AC129365.1	-
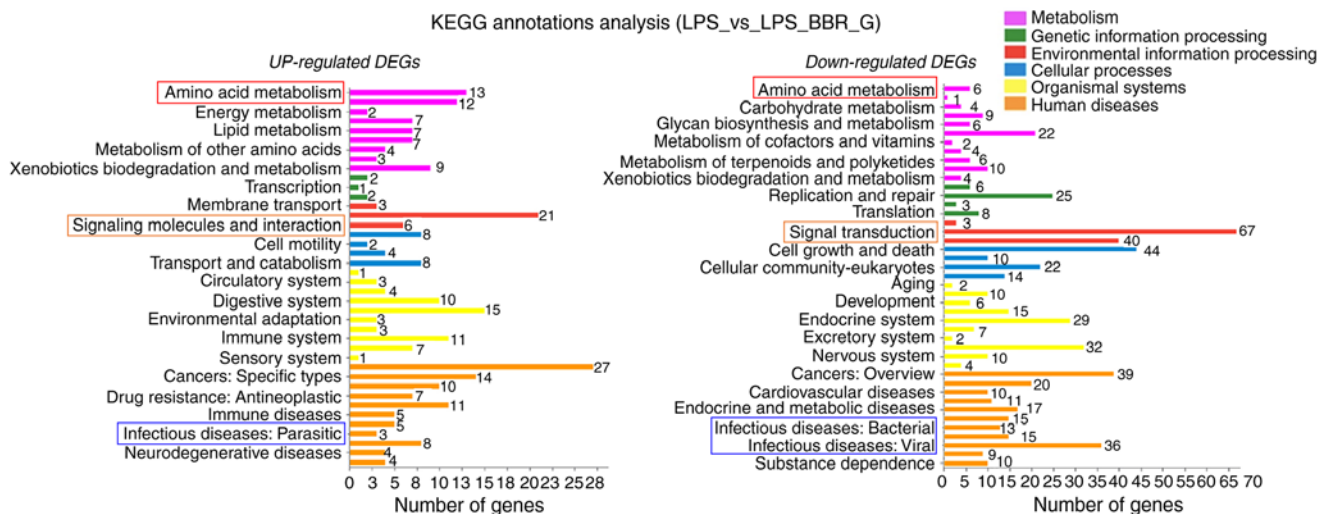
Figure 5. KEGG annotations analysis. The DEGs between LPS and LPS+BBR groups were classified into 'Metabolism', 'Genetic Information Processing', 'Environmental Information Processing', 'Cellular Processes', 'Organismal Systems' and 'Human Diseases'. Upregulated gene enrichment is shown on the left and downregulated gene enrichment on the right (red rectangle, 'amino acid metabolism'; orange rectangle, 'signaling molecules and interaction'; blue rectangle, 'infectious diseases'). DEGs, differentially expressed genes; LPS, lipopolysaccharide; BBR, berberine; KEGG, Kyoto Encyclopedia of Genes and Genomes.

Genes involved in apoptosis. A total of 19 genes associated with apoptosis were detected with significantly different expression levels, comparing between the LPS and BBR groups (13 were downregulated, whereas 6 were upregulated,
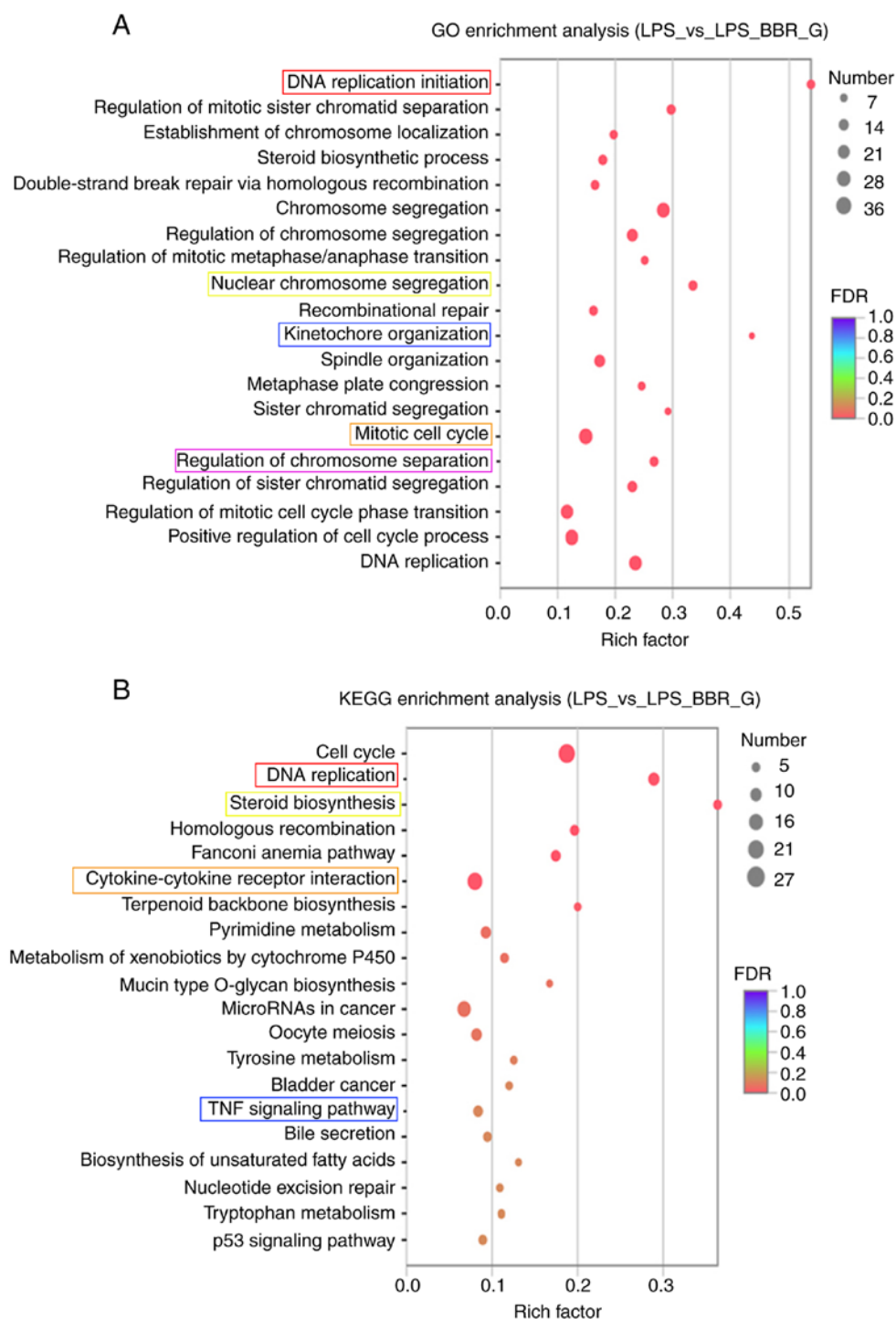
Figure 6. GO and KEGG enrichment analysis. (A) Top 20 ranked GO terms of DEGs between LPS and LPS+BBR groups (red rectangle, 'DNA replication initiation'; yellow rectangle, 'Nuclear chromosome segregation'; blue rectangle, 'Kinetochore organization'; orange rectangle, 'Mitotic cell cycle'; pink rectangle, 'Regulation of chromosome separation'). (B) Top 20 ranked KEGG pathways of DEGs between LPS and LPS+BBR groups (red rectangle, 'DNA replication'; yellow rectangle, 'Steroid biosynthesis'; orange rectangle, 'Cytokine-cytokine receptor interaction'; blue rectangle, 'TNF signaling pathway'). DEGs, differentially expressed genes; LPS, lipopolysaccharide; BBR, berberine; KEGG, Kyoto Encyclopedia of Genes and Genomes; GO, Gene Ontology.

in the BBR group) (Table III). The results of the present study indicated that the expression levels of cathepsin W (Ctsw), inhibitors of apoptosis proteins (IAPs)-Birc5 and Bcl-2 were downregulated, whereas cytochrome c testis (Cyct) and Bax were upregulated, in the BBR group compared with the LPS group, which suggested that, in the BBR group, more Cyct is released from mitochondria into the cytosol of numerous cell types undergoing apoptosis. Furthermore, a higher level of

caspase activation would result from the binding of Cyct to apoptotic protease-activating factor 1 and pro-caspase 9, thus promoting the formation of apoptosomes (29).

Genes involved in the TLR4/NF-κB and MAPK/AP-1 pathway. A total of 56 genes associated with inflammation were detected that had significantly different expression levels comparing between the BBR and LPS groups (47 were downregulated,
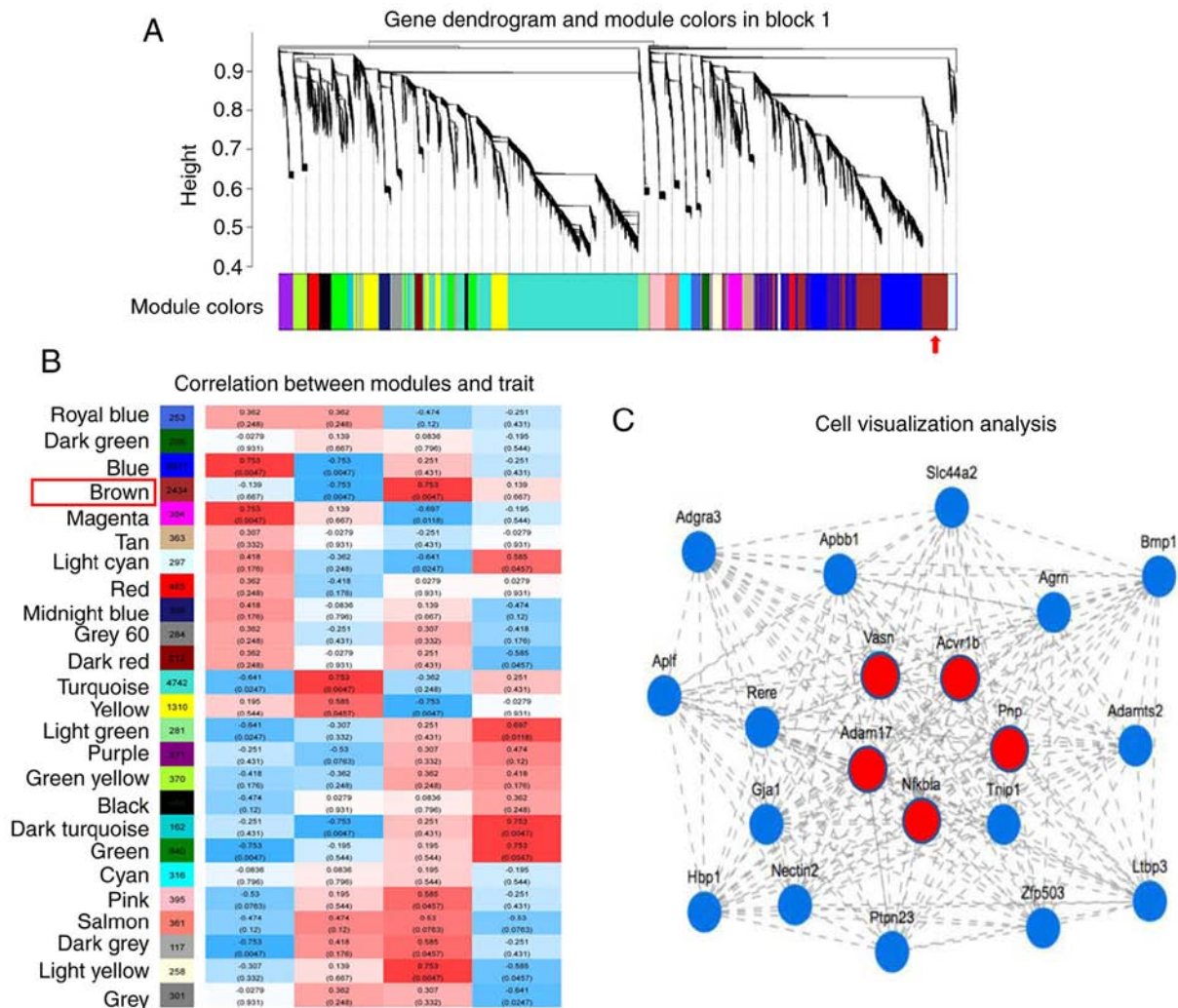
Figure 7. Weighted Gene Correlation Network Analysis. (A) A total of 32,883 genes were divided into 25 modules according to the similarity in expression patterns (the arrow points to the brown module). (B) The correlation between modules and groups. The abscissa represents different groups, and the ordinate represents different modules. A column of numbers on the left of the figure represents the number of genes of the module, and each set of data on the right represents the correlation coefficient and P-value of the module and group. Red indicates a greater correlation between module and group, whereas blue indicates a smaller correlation between module and group (red rectangle, module 'brown', the correction index is 0.753). (C) The top 20 hub genes of 'brown' module were obtained through the visualization network analysis, and the top 5 are labeled in red (Vasn, Adam17, Nfkbia, Pnp, Acvr1b). Vasn, Vasorin; Acvr1b, activin receptor type-1B; Nfkbia, NF-κB inhibitor α; Pnp, purine nucleoside phosphorylase; Adam17, disintegrin and metalloprotinease domain-containing protein 17.

whereas 9 were upregulated, in the BBR group) (Table IV). The results of the present study demonstrated that the expression levels of TLR4, myeloid differentiation primary response protein MyD88 (MyD88), TNF receptor-associated factor 6 (TRAF6), interleukin-1 receptor-associated kinase (IRAK)4, IRAK1, transforming growth factor-β-activated kinase (TAK)1, mitogen-activated protein kinase kinase (MKK)3, proto-oncogene c-Fos (c-Fos), c-Jun, MKK7, MAPK1 and MAPK3 were downregulated in the BBR group compared with the LPS group (Fig. 10B), suggesting that 'classical' inflammatory pathways, such as the TLR4/NF-κB and MAPK/AP-1 pathways, were inhibited by BBR (Fig. 10A).

Genes involved in leukocyte migration. A total of 16 genes associated with leukocyte migration were detected with significantly different expression levels, comparing between the BBR and LPS groups (all downregulated in the BBR group) (Table V). The results of the present study revealed that C-X-C motif chemokine

(Cxcl)1, Cxcl2, Cxcl3, Cxcl11, Cxcl9, C-C motif chemokine (Ccl)2, Ccl12, integrin a-M, vascular cell adhesion molecule 1 (Vcam1), Claudin-1, Cx3cl1 and intercellular cell adhesion molecule 1 (Icam1) were downregulated in the BBR group compared with the LPS group, suggesting that BBR is able to inhibit leukocyte migration via inhibiting chemokines and cell adhesion molecules, thereby reducing the infiltration of inflammatory cells and the harmful immune inflammatory response.

Discussion

The biomolecular events of DNA replication are central to diverse cellular processes, including development, cancer etiology, drug treatment and resistance (30). Numerous proteins and pathways exist to ensure the fidelity of DNA replication and protection of stalled or damaged replication forks. Consistently, mutations in proteins involved in DNA replication are implicated in diverse diseases that include defects
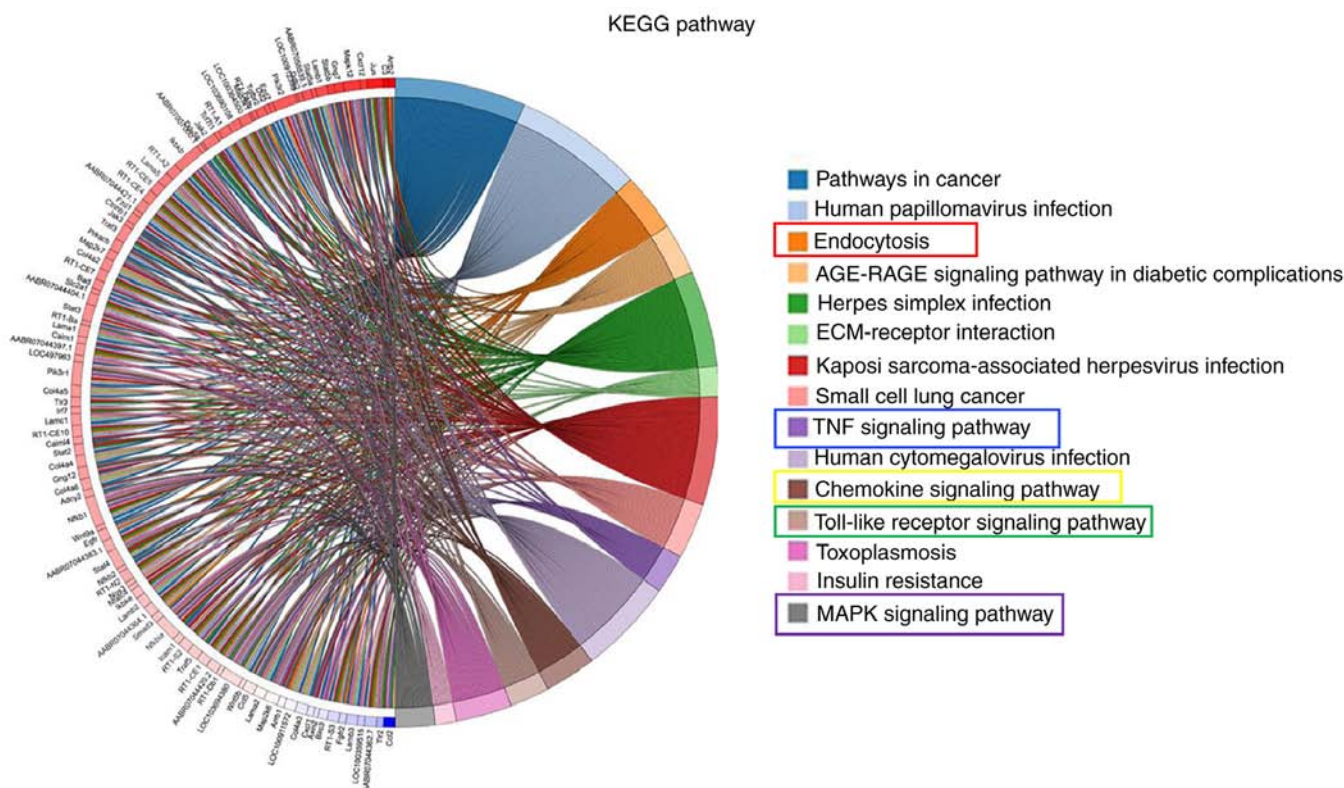
Figure 8. Gene enrichment chord analysis. Genes involved in module 'brown' were analyzed via KEGG enrichment analysis (red rectangle, 'Endocytosis'; blue rectangle, 'TNF signaling pathway'; yellow rectangle, 'Chemokine signaling pathway'; green rectangle, 'Toll-like receptor signaling pathway'; purple rectangle, 'MAPK signaling pathway'). KEGG, Kyoto Encyclopedia of Genes and Genomes.

during embryonic development and immunity, accelerated aging, increased inflammation, blood disease and cancer (23).

Precise duplication of genomic DNA is essential to maintain genome stability and prevent genetic abnormalities associated with cancer and other diseases. Accordingly, DNA replication includes an ordered and highly regulated series of steps, both before and during S phase (31). In preparation for S phase, DNA replication origins are generated in a process termed replication licensing, which occurs during late mitosis and G1. During this process, the ORC is recruited to specific genomic sites, where it binds and recruits the ATPase CDC6 and chromatin licensing and DNA replication factor 1, forming the pre-RC, which, in turn, facilitates the loading of the heterohexameric MCM2-7 complex onto chromatin (32-34). Once S phase begins, the MCM complex is activated to serve as the replicative helicase in association with CDC45 and DNA replication complex GINS protein PSF1, unwinding DNA at the replication fork (35,36). The replication fork is then loaded with proliferating cell nuclear antigen, a sliding processivity clamp for DNA synthesis in association with the replicative polymerases DNA polymerase d catalytic subunit and DNA polymerase e catalytic subunit A (37). Once replication is initiated at a given origin, the MCM helicase is displaced ahead of the replication fork, and is therefore never associated with newly replicated DNA (38).

Cell cycle activation (CCA) occurs in secondary injury after traumatic brain injury (TBI) (39). In postmitotic cells, such as neurons, CCA contributes to programmed cell death. In glia, CCA induces astrocyte and microglial proliferation/reactivation, leading to astroglial scar formation, the release of pro-inflammatory cytokines and reactive oxygen species (ROS), and, ultimately, neuronal degeneration (33-40). Administration of cell cycle inhibitors following TBI increases neuronal survival and reduces microglial and astroglial activation (41).

Previous studies have demonstrated that BBR induces significant mitochondrial apoptosis, G0/G1 cell cycle arrest and inhibitive migration in thyroid carcinoma cells via the phosphoinositide 3-kinase/AKT and MAPK signaling pathways (42). According to the transcriptome data in the present study, it is possible to hypothesize that BBR is able to influence the expression of key proteins, such as CDC6, ORC, MCM, CDC7, CycA, CycE and E2F, in the DNA replication process to cause cell cycle arrest.

Previous studies have revealed that ROS damage is the primary cause of cell death: The overexpression of Bcl-2 can reduce the production of oxygen radicals and the formation of lipid peroxides (43). These results suggest that the antioxidant effect of Bcl-2 is indirect; that is, it may lie in inhibiting the production of superoxide anions rather than in directly eliminating ROS (44). Cyt c is an important electron transporter in the respiratory chain. The release of Cyt c from the inner membrane of mitochondria blocks the function of the respiratory chain, leading to an accelerated production of superoxide anions (45). However, Bcl-2 is able to inhibit the release of Cyt c, thus inhibiting the production of superoxide anion (46). In addition, Bcl-2 can also increase the level of intracellular glutathione (GSH) and other antioxidants, increase the NAD/NADH ratio, inhibit the decrease of apoptosis-associated GSH and promote the entry of GSH into the nucleus, thereby affecting the redox state of cells (47). Programmed cell death,
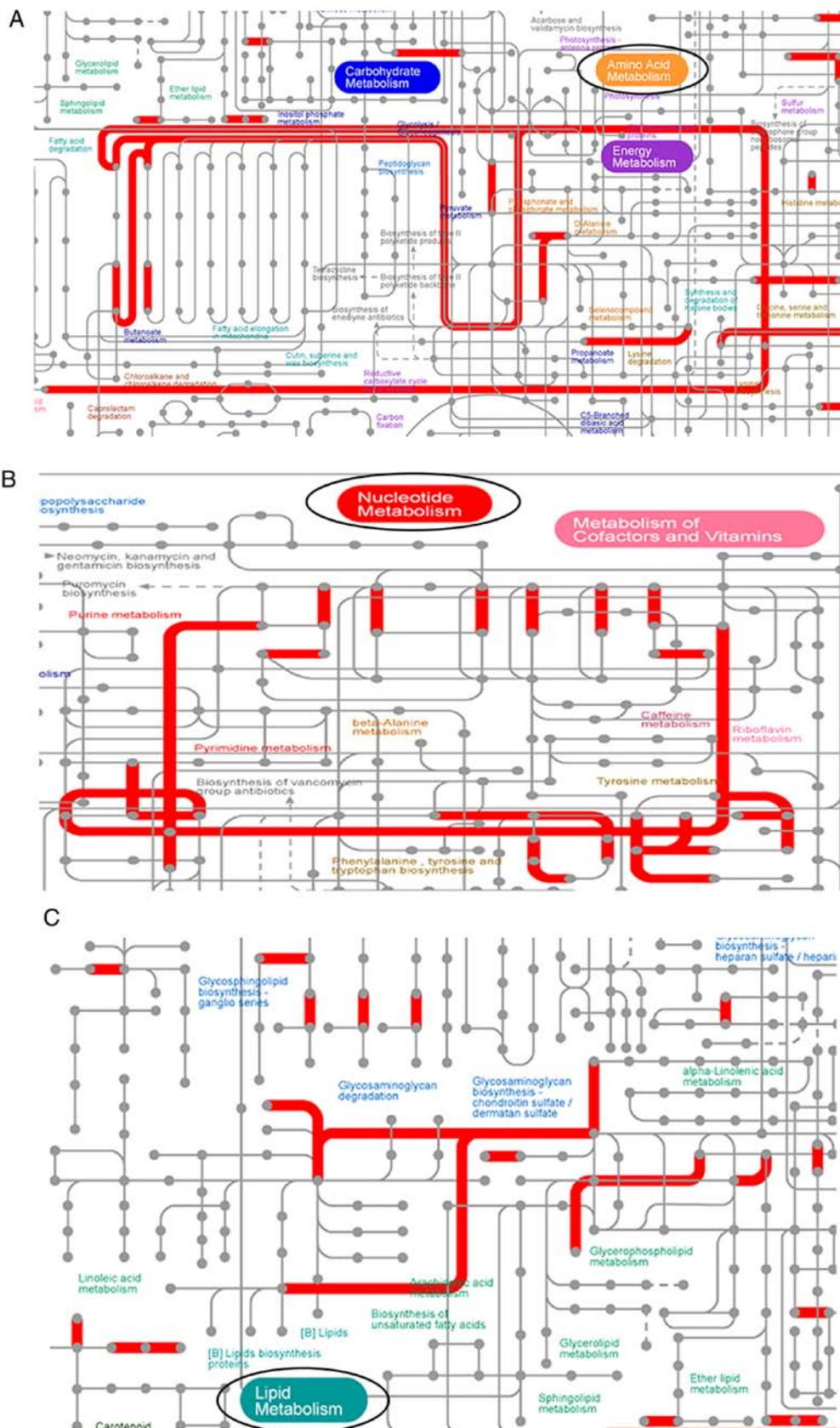
Figure 9. Interactive Pathways Explorer analysis. By visualizing the metabolic pathways involved in the DEGs between LPS and LPS + berberine groups, the red metabolic pathways were enriched by DEGS. (A) 'Amino acid metabolism' (black circle). (B) 'Nucleotide metabolism' (black circle). (C) 'Lipid metabolism' (black circle). DEGs, differentially expressed genes; LPS, lipopolysaccharide.

or apoptosis, is a major regulator of cell number and tissue homeostasis (48). Apoptosis is tightly controlled through the action of both activators and inhibitors of caspases (49). The best studied family of caspase inhibitors are the IAPs. Nitric

Table III. Genes involved in apoptosis.

LPS_vs._LPS_BBR (regulate)	Gene ID	Gene name	Gene description
Down	ENSRNOG00000013774	Lmnb1	Lamin B1
Down	ENSRNOG00000007529	Bmf	Bcl2 modifying factor
Down	ENSRNOG00000016571	Ngf	Nerve growth factor
Down	ENSRNOG00000027096	Ctsw	Cathepsin W
Down	ENSRNOG00000050819	Birc5	Baculoviral IAP repeat-containing 5
Down	ENSRNOG00000003537	Spta1	Spectrin α erythrocytic 1
Down	ENSRNOG00000002791	Bcl-2	BCL2 apoptosis regulator
Down	ENSRNOG00000022521	Ddias	DNA damage-induced apoptosis suppressor
Down	ENSRNOG00000007367	Sept4	Septin 4
Down	ENSRNOG00000058834	LOC103692471	Uncharacterized LOC103692471
Down	ENSRNOG00000053339	AABR07062512.1	-
Down	ENSRNOG00000012473	Cflar	CASP8 and FADD-like apoptosis regulator
Down	ENSRNOG00000060728	Tuba1a	Tubulin α1A
Up	ENSRNOG00000023463	Parp9	Poly (ADP-ribose) polymerase family member 9
Up	ENSRNOG00000003084	Parp1	Poly (ADP-ribose) polymerase 1
Up	ENSRNOG00000008892	Parp2	Poly (ADP-ribose) polymerase 2
Up	ENSRNOG00000024457	Cyt c	Cytochrome c testis
Up	ENSRNOG00000020876	Bax	BCL2 associated X apoptosis regulator
Up	ENSRNOG00000007529	Bmf	Bcl2 modifying factor

oxide (NO)-induced apoptosis is associated with the down-regulation of IAP expression, which facilitates the activation of the caspase cascade and subsequent poly-ADP-ribose polymerase (PARP) cleavage (50).

A previous study reported that, in cells treated with BBR, the expression levels of Bax and PARP cleavage were increased, whereas the expression level of Bcl-2 was reduced (51). BBR has also been demonstrated to induce dose-dependent quiescence and apoptosis in A549 cancer cells through modulating cell cyclins and inflammation independently of the mTOR pathway (52). The results of the present study were consistent with these previous reports. According to the transcriptome data of the present study, it was possible to speculate that BBR may regulate Bax/Bcl-2 gene expression by downregulating cathepsin and IAPs, causing mitochondria to release excessive levels of Cyt c that induce apoptosis, thereby combatting inflammatory damage.

In previous studies, BBR has been found to be able to inhibit LPS-induced expression of inflammatory cytokines by suppressing the TLR4-mediated NF-κB and MAPK signaling pathways in rumen epithelial cells (53). BBR was also reported to inhibit AP-1 activity in a dose- and time-dependent manner. BBR concentrations as low as $10 \mu M$ were found to inhibit AP-1 activity almost completely following 48 h treatment (54). These results, together with those of the present study, demonstrate that BBR exerts a significant influence on the TLR4/NF-κB and MAPK/AP-1 pathway. The transcriptome data of the present study revealed the role of BBR in both pathways more comprehensively, further clarifying the functional genes that are located upstream or downstream in these pathways. According to a previous study, the TLR4-mediated response to

LPS can be divided into two types: An early MyD88-dependent response and a delayed MyD88-independent response (55). Downstream events in the activation of the MyD88-dependent pathway are elicited by LPS, leading to activation of the NF-κB and MAPK pathways. A typical model of the activation of NF-κB is initiated by the binding of IRAK-1 and IRAK-4 to the receptor complex. The phosphorylation of IRAK-1 occurs in two substeps, giving rise to hyperphosphorylated IRAK-1, which separates IRAK-1 from the receptor complex, causing it to bind with TRAF6 (56). TRAF6 subsequently becomes activated and associates with TGF-β-activated kinase 1 MAP3K7-binding protein (TAB)2 to activate the MAPK kinase, TAK1, which is constitutively associated with its adaptor protein, TAB-1 (57,58). At this point, TAK-1 acts as a common activator of NF-κB, as well as of the c-Jun N-terminal kinase (JNK) and p38 pathways (59). The activation of NF-κB is initiated by the assembly of a high-molecular-weight protein complex known as the signalosome. This complex comprises IKKα and IKKβ, together with a scaffolding protein named IKKγ (also known as NEMO). Subsequent phosphorylation of a set of IκBs results in their degradation and ubiquitination, releasing NF-κB factor, which can then translocate to the nucleus. MAPKs are highly conserved protein threonine/serine kinases, and three major subfamilies, including extracellular signal-regulating kinases (ERKs) 1 and 2, JNK and p38, have been found in mammalian cells (59-61). MAPKs have been demonstrated to be involved in pro-inflammatory signaling pathways, and abundant evidence has demonstrated that the activation of ERK1/2, JNK and p38 is involved in the upregulation of TNF-α, inducible nitric oxide synthase, IL-6 and COX-2 in LPS-activated macrophages. ERK1/2 and JNK

Table IV. Genes involved in the TLR4/NF-kB and MAPK/AP-1 pathways.

LPS_vs._LPS_BBR	Gene ID	Gene name	Gene description
Down	ENSRNOG00000007390	Nfkbia	NFKB inhibitor α
Down	ENSRNOG00000008859	Tank	TRAF family member-associated NFKB activator
Down	ENSRNOG00000008565	Nkiras1	NFKB inhibitor interacting Ras-like 1
Down	ENSRNOG00000053813	Nkap	NFKB activating protein
Down	ENSRNOG00000061989	Nkrf	NFKB repressing factor
Down	ENSRNOG00000005965	Irak4	interleukin-1 receptor-associated kinase 4
Down	ENSRNOG00000020063	Nfkbib	NFKB inhibitor β
Down	ENSRNOG00000025111	Nfkbid	NFKB inhibitor δ
Down	ENSRNOG00000016010	Mul1	Mitochondrial E3 ubiquitin protein ligase 1
Down	ENSRNOG00000019907	Nfkbie	NFKB inhibitor ε
Down	ENSRNOG00000056708	Nkapl	NFKB activating protein-like
Down	ENSRNOG00000004639	Traf6	TNF receptor associated factor 6
Down	ENSRNOG00000023258	Nfkb1	Nuclear factor κB subunit 1
Down	ENSRNOG00000018095	Nkiras2	NFKB inhibitor interacting Ras-like 2
Down	ENSRNOG00000000839	Nfkbil1	NFKB inhibitor like 1
Down	ENSRNOG00000014703	Tonsl	Tonsoku-like DNA repair protein
Down	ENSRNOG00000019311	Nfkb2	Nuclear factor κB subunit 2
Down	ENSRNOG00000060869	Irak1	Interleukin-1 receptor-associated kinase 1
Down	ENSRNOG00000010522	Tlr4	Toll-like receptor 4
Down	ENSRNOG00000019073	Ikbkb	Inhibitor of nuclear factor κB kinase subunit β
Down	ENSRNOG00000007159	Ccl2	C-C motif chemokine ligand 2
Down	ENSRNOG00000004553	Cox2	Cytochrome c oxidase assembly factor COX2
Down	ENSRNOG00000014454	Ap1m1	Adaptor related protein complex 1 subunit μ1
Down	ENSRNOG00000002061	Ptpn13	Protein tyrosine phosphatase non-receptor type
Down	ENSRNOG00000038686	Ap1s2	Adaptor related protein complex 1 subunit σ2
Down	ENSRNOG00000001415	Ap1s1	Adaptor related protein complex 1 subunit σ1
Down	ENSRNOG00000061543	Ap2b1	Adaptor related protein complex 2 subunit β1
Down	ENSRNOG00000013634	Myd88	MYD88 innate immune signal transduction adaptor
Down	ENSRNOG00000012701	Map7	Microtubule-associated protein 7
Down	ENSRNOG00000019568	Jund	JunD proto-oncogene AP-1 transcription factor subunit
Down	ENSRNOG00000029456	Rp9	RP9 pre-mRNA splicing factor
Down	ENSRNOG00000013690	Clba1	Clathrin binding box of aftiphilin containing 1
Down	ENSRNOG00000027831	Map7d3	MAP7 domain containing 3
Down	ENSRNOG00000047516	Map3k7	Mitogen activated protein kinase kinase kinase 7
Down	ENSRNOG00000005411	Aftph	Aftiphilin
Down	ENSRNOG00000032463	Rap1a	RAP1A member of RAS oncogene family
Down	ENSRNOG00000008786	Ap1b1	Adaptor related protein complex 1 subunit β1
Down	ENSRNOG00000020552	Fosl1	FOS like 1 AP-1 transcription factor subunit
Down	ENSRNOG00000001849	Mapk1	Mitogen activated protein kinase 1
Down	ENSRNOG00000053583	Mapk3	Mitogen activated protein kinase 3
Down	ENSRNOG00000010237	Map7d1	MAP7 domain containing 1
Down	ENSRNOG00000046667	Fosb	FosB proto-oncogene AP-1 transcription factor subunit
Down	ENSRNOG00000006789	Ddit3	DNA-damage inducible transcript 3
Down	ENSRNOG00000005176	Map7d2	MAP7 domain containing 2
Down	ENSRNOG00000007048	Rap1b	RAP1B member of RAS oncogene family
Down	ENSRNOG00000026293	Jun	Jun proto-oncogene AP-1 transcription factor subunit
Down	ENSRNOG00000024492	Ap1ar	Adaptor-related protein complex 1 associated regulatory protein
Up	ENSRNOG00000014258	Rab32	RAB32 member RAS oncogene family
Up	ENSRNOG00000049873	Ap1s3	Adaptor related protein complex 1 subunit σ3
Up	ENSRNOG00000017871	Sidt2	SID1 transmembrane family member 2
Up	ENSRNOG00000052357	Fosl2	FOS like 2 AP-1 transcription factor subunit

Table IV. Continued.

LPS_vs._LPS_BBR	Gene ID	Gene name	Gene description
Up	ENSRNOG00000000151	Ldlrap1	Low density lipoprotein receptor adaptor protein 1
Up	ENSRNOG00000016769	Rab38	RAB38 member RAS oncogene family
Up	ENSRNOG00000042838	Junb	JunB proto-oncogene AP-1 transcription factor subunit
Up	ENSRNOG00000025619	Ap1g2	Adaptor related protein complex 1 subunit γ2
Up	ENSRNOG00000008015	Fos	Fos proto-oncogene AP-1 transcription factor subunit

Table V. Genes involved in leukocyte migration.

LPS_vs._LPS_BBR	Gene ID	Gene name	Gene description
Down	ENSRNOG00000014333	Vcam1	Vascular cell adhesion molecule 1
Down	ENSRNOG00000019728	Itgam	Integrin subunit αM
Down	ENSRNOG00000017539	Mmp9	Matrix metallopeptidase 9
Down	ENSRNOG00000001926	Cldn1	Claudin 1
Down	ENSRNOG00000006984	Mapk11	Mitogen-activated protein kinase 11
Down	ENSRNOG00000016695	Mmp2	Matrix metallopeptidase 2
Down	ENSRNOG00000020246	Myl9	Myosin light chain 9
Down	ENSRNOG00000022298	Cxcl11	C-X-C motif chemokine ligand 11
Down	ENSRNOG00000028043	Cxcl3	Chemokine (C-X-C motif) ligand 3
Down	ENSRNOG00000002792	Cxcl2	C-X-C motif chemokine ligand 2
Down	ENSRNOG00000002802	Cxcl1	C-X-C motif chemokine ligand 1
Down	ENSRNOG00000022242	Cxcl9	C-X-C motif chemokine ligand 9
Down	ENSRNOG00000007159	Ccl2	C-C motif chemokine ligand 2
Down	ENSRNOG00000029768	Ccl12	Chemokine (C-C motif) ligand 12
Down	ENSRNOG00000016326	Cx3cl1	C-X3-C motif chemokine ligand 1
Down	ENSRNOG00000020679	Icam1	Intercellular adhesion molecule 1

then promote the combination of c-Jun and c-Fos, which in turn activates AP-1 (62).

Directional migration of leukocytes is crucial in innate immunity for host defense. However, the recruitment of leukocytes at the site of tissue injury are a leading cause of the inflammatory response (63). Chemokines have emerged as the most important regulators of leukocyte trafficking during inflammation. A number of chemokines have been implicated in the pathogenesis of IBD (64). Upon detecting external stimuli, IECs have the potential to secrete chemokines that can recruit immune cells and directly induce the secretion of inflammatory cytokines, which augment and prolong inflammatory responses. For example, CXCL8, which is secreted from IECs and immune cells and is considered to be a major chemotactic factor, can attract C-X-C chemokine receptor type (CXCR)1(+)/CXCR2(+) IL-23-producing neutrophils that infiltrate and accumulate in inflamed colon tissue (65). ICAM-1 and VCAM-1 are two important members of the immunoglobulin gene superfamily, although they have different roles in the adhesion of leukocytes to the vascular endothelium. ICAM-1 can promote adhesion at the site of inflammation, thereby controlling cancer progression and regulating immune responses in the tissue. These membrane proteins are necessary for anchoring leukocytes to

the vessel wall (66). Upregulated expression of claudin-1, which is involved in early stages of transformation in IBD-associated neoplasia (67). At present, few studies have been conducted on the potential anti-inflammatory ability of BBR in downregulating the expression of chemokines.

Previous studies have demonstrated that BBR was able to reverse chronic inflammatory pain induced by Complete Freund's adjuvant, which alleviated comorbid depression (68,69). Its anti-nociceptive and anti-depressive effects may be associated with the downregulated spinal levels of the inflammatory cytokines and mRNA transcription of CCL2 (70). The results of the present study showed that the anti-inflammatory mechanism of BBR is likely to be associated with the regulation of chemokines and the migration of leukocytes, which may provide a novel perspective for future studies.

Recently, a large number of publications have focused on the relationship between host metabolism and inflammation (71,72). Atherosclerosis is a lipid- and immune cell-driven chronic inflammatory disease that is characterized by endothelial dysfunction and defective non-revolving immune responses. Arginine, L-homoarginine and L-tryptophan metabolism have been revealed to exert an influence on
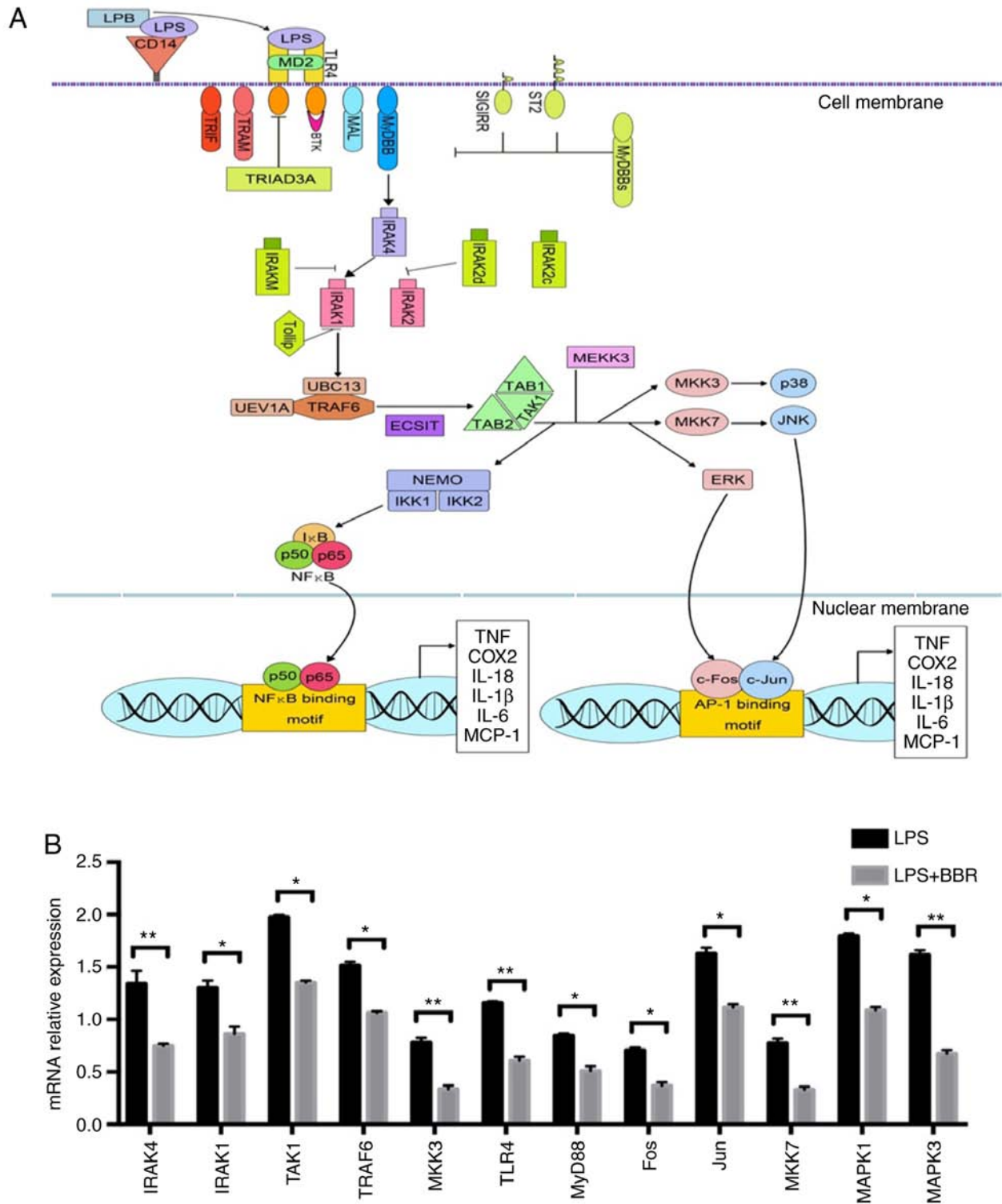
Figure 10. Anti-inflammatory effects of BBR on LPS-induced inflammation via suppression of the TLR4/NF-κB and MAPK/AP-1 pathways. (A) Based on the transcriptome data and Kyoto Encyclopedia of Genes and Genomes pathway database, a diagram of the TLR4/NF-κB and MAPK/AP-1 pathways was constructed. (B) Reverse transcription-quantitative PCR was used to verify the key genes, including IRAK4, IRAK1, TAK1, TRAF6, MKK3, TLR4, MyD88, c-Fos, c-Jun, MKK7, MAPK1 and MAPK3 in IEC-18 cells, the results were analyzed by an unpaired t-test with GraphPad 8.0 software. $^*P<0.05$ and $^{**}P<0.01$. LPS, lipopolysaccharide; BBR, berberine; TLR4, toll-like receptor 4; MyD88, myeloid differentiation primary response protein; IRAK4, interleukin-1 receptor-associated kinase; TAK1, transforming growth factor-β-activated kinase 1; TRAF6, TNF receptor-associated factor 6; MKK3, mitogen-activated protein kinase kinase 3; c-Fos, proto-oncogene c-Fos.

immune regulation in endothelial, as well as innate and adaptive immune cells, and their metabolites may be considered as putative therapeutic targets in chronic inflammatory disease (73). Whey protein hydrolysate and branched-chain

amino acids downregulate inflammation-associated genes in vascular endothelial cells (74). The iPath metabolic network analysis of the present study revealed the potential association between BBR and amino acid metabolism, nucleotide

metabolism and lipid metabolism, which may provide a new explanation for BBR's anti-inflammatory effects.

BBR has already been approved for clinical therapy in China, and a recent large-scale double-blind clinical trial has reported that BBR is safe and effective to prevent colorectal cancer (75). However, BBR has not been approved by FDA since the mechanism underlying its anti-inflammatory activity remains poorly understood. As an anti-inflammatory drug, its targets and mechanisms are complex and diverse, so it is necessary to study the drug from a wide range of different perspectives. In addition to the classical regulation of gene expression, it is now possible to explain the action of BBR at the level of metabolism or the level of intestinal microorganisms. Despite some significant progress that has been made in this regard with the findings of the present study, there were also certain limitations; for example, not having set multiple sampling time points and drug concentrations. Also, the results of this study would be more meaningful if samples from animals or human IECs had been used. Therefore, it is necessary to perform an in-depth exploration of this topic in the future.

Acknowledgements

Availability of data and materials

The datasets generated during the current study are available in the National Center for Biotechnology Information database: ncbi.nlm.nih.gov/ [SRP254018].

Authors' contributions

XX, LZ, YZ and LM designed the experiment. XX, BX, WQ, YY, CX and BY analyzed the data. XX and LM wrote and revised the article. All authors read and approved the final manuscript.

Ethics approval and consent to participate

Not applicable.

Patient consent for publication

Not applicable.

Competing interests

The authors declare that they have no competing interests.

References

1. Fest J, Ruiter R, Mulder M, Groot Koerkamp B, Ikram MA, Stricker BH and van Eijck CHJ: The systemic immune-inflammation index is associated with an increased risk of incident cancer-A population-based cohort study. Int J Cancer 146: 692-698, 2020.

2. Das S, Reddy MA, Senapati P, Stapleton K, Lanting L, Wang M, Amaram V, Ganguly R, Zhang L, Devaraj S, *et al*: Diabetes mellitus-induced long noncoding RNA Dnm3os regulates macrophage functions and inflammation via nuclear mechanisms. Arterioscler Thromb Vasc Biol 38: 1806-1820, 2018.

3. Sorriento D and Iaccarino G: Inflammation and cardiovascular diseases: The most recent findings. Int J Mol Sci 20: 3879, 2019.

4. Dragasevic S, Stankovic B, Kotur N, Sokic-Milutinovic A, Milovanovic T, Lukic S, Milosavljevic T, Srzentic Drazilov S, Klaassen K, Pavlovic S and Popovic D: Metabolic syndrome in inflammatory bowel disease: Association with genetic markers of obesity and inflammation. Metab Syndr Relat Disord 18: 31-38, 2020.

5. Bian Y, Dong Y, Sun J, Sun M, Hou Q, Lai Y and Zhang B: Protective effect of kaempferol on LPS-induced inflammation and barrier dysfunction in a coculture model of intestinal epithelial cells and intestinal microvascular endothelial cells. J Agric Food Chem 68: 160-167, 2020.

6. Huttenhower C, Kostic AD and Xavier RJ: Inflammatory bowel disease as a model for translating the microbiome. Immunity 40: 843-854, 2014.

7. Vong LB, Mo J, Abrahamsson B and Nagasaki Y: Specific accumulation of orally administered redox nanotherapeutics in the inflamed colon reducing inflammation with dose-response efficacy. J Control Release 210: 19-25, 2015.

8. Aziz DA, Moin M, Majeed A, Sadiq K and Biloo AG: Paediatric inflammatory bowel disease: Clinical presentation and disease location. Pak J Med Sci 33: 793-797, 2017.

9. Peterson LW and Artis D: Intestinal epithelial cells: Regulators of barrier function and immune homeostasis. Nat Rev Immunol 14: 141-153, 2014.

10. Allaire JM, Crowley SM, Law HT, Chang SY, Ko HJ and Vallance BA: The intestinal epithelium: Central coordinator of mucosal immunity. Trends Immunol 39: 677-696, 2018.

11. Zeng XZ, Zhang YY, Yang Q, Wang S, Zou BH, Tan YH, Zou M, Liu SW and Li XJ: Artesunate attenuates LPS-induced osteoclastogenesis by suppressing TLR4/TRAF6 and PLCγ1-Ca $^{2+}$-NFATc1 signaling pathway. Acta Pharmacol Sin 41: 229-236, 2020.

12. Fang F and Jiang D: IL-1β/HMGB1 signalling promotes the inflammatory cytokines release via TLR signalling in human intervertebral disc cells. Biosci Rep 36: e00379, 2016.

13. Yeh M, Granger DN and Glass J: Increases in IKK-A activity, IKB-A phosphorylation and degradation and p50 subunit production precede nfkb activation in the intestine of rats after LPS administration. Gastroenterology 118: PA819, 2000.

14. Shirwaikar A, Shirwaikar A, Rajendran K and Punitha IS: In vitro antioxidant studies on the benzyl tetra isoquinoline alkaloid berberine. Biol Pharm Bull 29: 1906-1910, 2006.

15. Tang J, Feng Y, Tsao S, Wang N, Curtain R and Wang Y: Berberine and Coptidis rhizoma as novel antineoplastic agents: A review of traditional use and biomedical investigations. J Ethnopharmacol 126: 5-17, 2009.

16. Germoush MO and Mahmoud AM: Berberine mitigates cyclophosphamide-induced hepatotoxicity by modulating antioxidant status and inflammatory cytokines. J Cancer Res Clin Oncol 140: 1103-1109, 2014.

17. Liu YF, Wen CY, Chen Z, Wang Y, Huang Y and Tu SH: Effects of berberine on NLRP3 and IL-1β expressions in monocytic THP-1 cells with monosodium urate crystals-induced inflammation. Biomed Res Int 2016: 2503703, 2016.

18. Kuo CL, Chi CW and Liu TY: The anti-inflammatory potential of berberine in vitro and in vivo. Cancer Lett 203: 127-137, 2004.

19. Bae YA and Cheon HG: Activating transcription factor-3 induction is involved in the anti-inflammatory action of berberine in RAW264.7 murine macrophages. Korean J Physiol Pharmacol 20: 415-424, 2016.

20. Zhang H, Shan Y, Wu Y, Xu C, Yu X, Zhao J, Yan J and Shang W: Berberine suppresses LPS-induced inflammation through modulating Sirt1/NF-κB signaling pathway in RAW264.7 cells. Int Immunopharmacol 52: 93-100, 2017.

21. Li H, Fan C, Lu H, Feng C, He P, Yang X, Xiang C, Zuo J and Tang W: Protective role of berberine on ulcerative colitis through modulating enteric glial cells-intestinal epithelial cells-immune cells interactions. Acta Pharm Sin B 10: 447-461, 2020.

22. Jing W, Safarpour Y, Zhang T, Guo P, Chen G, Wu X, Fu Q and Wang Y: Berberine upregulates P-Glycoprotein in human caco-2 cells and in an experimental model of colitis in the rat via activation of Nrf2-dependent mechanisms. J Pharmacol Exp Ther 366: 332-340, 2018.

23. Li C, Xi Y, Li S, Zhao Q, Cheng W, Wang Z, Zhong J, Niu X and Chen G: Berberine ameliorates TNBS induced colitis by inhibiting inflammatory responses and Th1/Th17 differentiation. Mol Immunol 67: 444-454, 2015.
24. Pengyu Z, Yan Y, Xiying F, Maoguang Y, Mo L, Yan C, Hong S, Lijuan W, Xiujuan Z and Hanqing C: The differential expression of long noncoding RNAs in type 2 diabetes mellitus and latent autoimmune diabetes in adults. Int J Endocrinol 2020: 9235329, 2020.
25. Ashburner M, Ball CA, Blake JA, Botstein D, Butler H, Cherry JM, Davis AP, Dolinski K, Dwight SS, Eppig JT, et al: Gene ontology: Tool for the unification of biology. The gene ontology consortium. Nat Genet 25: 25-29, 2000.
26. The Gene Ontology Consortium: The gene ontology resource: 20 years and still GOing strong. Nucleic Acids Res 47: D330-D338, 2019.
27. Ogata H, Goto S, Sato K, Fujibuchi W, Bono H and Kanehisa M: KEGG: Kyoto encyclopedia of genes and genomes. Nucleic Acids Res 27: 29-34, 1999.
28. Chang S, Chen W and Yang J: Another formula for calculating the gene change rate in real-time RT-PCR. Mol Biol Rep 36: 2165-2168, 2009.
29. Zhang Y, Zhao L, Li X, Wang Y, Yao J, Wang H, Li F, Li Z and Guo Q: V8, a newly synthetic flavonoid, induces apoptosis through ROS-mediated ER stress pathway in hepatocellular carcinoma. Arch Toxicol 88: 97-107, 2014.
30. Mosmann T: Rapid colorimetric assay for cellular growth and survival: Application to proliferation and cytotoxicity assays. J Immunol Methods 65: 55-63, 1983.
31. Loeb LA and Monnat RJ Jr: DNA polymerases and human disease. Nature Rev Genet 9: 594-604, 2008.
32. Zeman MK and Cimprich KA: Causes and consequences of replication stress. Nat Cell Biol 16: 2-9, 2014.
33. Blow JJ and Gillespie PJ: Replication licensing and cancer-a fatal entanglement? Nat Rev Cancer 8: 799-806, 2008.
34. Mendez J and Stillman B: Perpetuating the double helix: Molecular machines at eukaryotic DNA replication origins. Bioessays 25: 1158-1167, 2003.
35. Blow JJ and Dutta A: Preventing re-replication of chromosomal DNA. Nature reviews. Nat Rev Mol Cell Biol 6: 476-486, 2005.
36. Arias EE and Walter JC: Strength in numbers: Preventing rereplication via multiple mechanisms in eukaryotic cells. Genes Dev 21: 497-518, 2007.
37. Moyer SE, Lewis PW and Botchan MR: Isolation of the Cdc45/Mcm2-7/GINS (CMG) complex, a candidate for the eukaryotic DNA replication fork helicase. Proc Natl Acad Sci USA 103: 10236-10241, 2006.
38. Ilves I, Petojevic T, Pesavento JJ and Botchan MR: Activation of the MCM2-7 helicase by association with Cdc45 and GINS proteins. Mol Cell 37: 247-258, 2010.
39. Moldovan GL, Pfander B and Jentsch S: PCNA, the maestro of the replication fork. Cell 129: 665-679, 2007.
40. Cernak I, Stoica B, Byrnes KR, Di Giovanni S and Faden AI: Role of the cell cycle in the pathobiology of central nervous system trauma. Cell Cycle 4: 1286-1293, 2005.
41. Stoica BA, Byrnes KR and Faden AI: Cell cycle activation and CNS injury. Neurotox Res 16: 221-237, 2009.
42. Li L, Wang X, Sharvan R, Gao J and Qu S: Berberine could inhibit thyroid carcinoma cells by inducing mitochondrial apoptosis, G0/G1 cell cycle arrest and suppressing migration via PI3K-AKT and MAPK signaling pathways. Biomed Pharmacother 95: 1225-1231, 2017.
43. Chong SJ, Low IC and Pervaiz S: Mitochondrial ROS and involvement of Bcl-2 as a mitochondrial ROS regulator. Mitochondrion 19: 39-48, 2014.
44. Hashemi-Niasari F, Rabbani-Chadegani A, Razmi M and Fallah S: Synergy of theophylline reduces necrotic effect of berberine, induces cell cycle arrest and PARP, HMGB1, Bcl-2 family mediated apoptosis in MDA-MB-231 breast cancer cells. Biomed Pharmacother 106: 858-867, 2018.
45. PLOS ONE Editors: Retraction: Bak compensated for bax in p53-null cells to release cytochrome c for the initiation of mitochondrial signaling during withanolide D-induced apoptosis. PLoS One 15: e0228839, 2020.
46. Neame SJ, Rubin LL and Philpott KL: Blocking cytochrome c activity within intact neurons inhibits apoptosis. J Cell Biol 142: 1583-1593, 1998.
47. Chauhan D, Pandey P, Ogata A, Teoh G, Krett N, Halgren R, Rosen S, Kufe D, Kharbanda S and Anderson K: Cytochrome c-dependent and -independent induction of apoptosis in multiple myeloma cells. J Biol Chem 272: 29995-29997, 1997.
48. Campisi L, Cummings RJ and Blander JM: Death-defining immune responses after apoptosis. Am J Transplant 14: 1488-1498, 2014.
49. Song Z and Steller H: Death by design: Mechanism and control of apoptosis. Trends Cell Biol 9: M49-M52, 1999.
50. Stanford A, Chen Y, Zhang XR, Hoffman R, Zamora R and Ford HR: Nitric oxide mediates dendritic cell apoptosis by downregulating inhibitors of apoptosis proteins and upregulating effector caspase activity. Surgery 130: 326-332, 2001.
51. Fu L, Chen W, Guo W, Wang J, Tian Y, Shi D, Zhang X, Qiu H, Xiao X, Kang T, et al: Berberine targets AP-2/hTERT, NF-κB/COX-2, HIF-1α/VEGF and Cytochrome-c/Caspase signaling to suppress human cancer cell growth. PLoS One 8: e69240, 2013.
52. Kalaiarasi A, Anusha C, Sankar R, Rajasekaran S, John Marshal J, Muthusamy K and Ravikumar V: Plant isoquinoline alkaloid berberine exhibits chromatin remodeling by modulation of histone deacetylase to induce growth arrest and apoptosis in the A549 cell line. J Agric Food Chem 64: 9542-9550, 2016.
53. Zhao O, Wang Y, Yuan X, Sun G, Shen B, Xu F, Fan G, Jin M, Li X and Liu G: Berberine inhibits lipopolysaccharide-induced expression of inflammatory cytokines by suppressing TLR4-mediated NF-κB and MAPK signaling pathways in rumen epithelial cells of Holstein calves. J Dairy Res 86: 171-176, 2019.
54. Kim S, Choi JH, Kim JB, Nam SJ, Yang JH, Kim JH and Lee JE: Berberine suppresses TNF-alpha-induced MMP-9 and cell invasion through inhibition of AP-1 activity in MDA-MB-231 human breast cancer cells. Molecules 13: 2975-2985, 2008.
55. Güney Eskiler G, Deveci Özkan A, Kaleli S and Bilir C: Inhibition of TLR4/TRIF/IRF3 signaling pathway by curcumin in breast cancer cells. J Pharm Pharm Sci 22: 281-291, 2019.
56. Muroi M and Tanamoto K: TRAF6 distinctively mediates MyD88- and IRAK-1-induced activation of NF-kappaB. J Leukoc Biol 83: 702-707, 2008.
57. Zhang J, Macartney T, Peggie M and Cohen P: Interleukin-1 and TRAF6-dependent activation of TAK1 in the absence of TAB2 and TAB3. Biochem J 474: 2235-2248, 2017.
58. Jang JH, Kim H and Cho JH: Molecular cloning and functional characterization of TRAF6 and TAK1 in rainbow trout, oncorhynchus mykiss. Fish Shellfish Immunol 84: 927-936, 2019.
59. Yu-Wei D, Li ZS, Xiong SM, Huang G, Luo YF, Huo TY, Zhou MH and Zheng YW: Paclitaxel induces apoptosis through the TAK1-JNK activation pathway. FEBS Open Bio 10: 1655-1667, 2020.
60. Yuan Z, Liang Z, Yi J, Chen X, Li R, Wu J and Sun Z: Koumine promotes ROS production to suppress hepatocellular carcinoma cell proliferation via NF-κB and ERK/p38 MAPK signaling. Biomolecules 9: 559, 2019.
61. Pan J, Jin R, Shen M, Wu R and Xu S: Acamprosate protects against adjuvant-induced arthritis in rats via blocking the ERK/MAPK and NF-κB signaling pathway. Inflammation 41: 1194-1199, 2018.
62. Kitanaka T, Nakano R, Kitanaka N, Kimura T, Okabayashi K, Narita T and Sugiya H: JNK activation is essential for activation of MEK/ERK signaling in IL-1β-induced COX-2 expression in synovial fibroblasts. Sci Rep 7: 39914, 2017.
63. Rossaint J, Margraf A and Zarbock A: Role of platelets in leukocyte recruitment and resolution of inflammation. Front Immunol 9: 2712, 2018.
64. Trivedi PJ and Adams DH: Chemokines and chemokine receptors as therapeutic targets in inflammatory bowel disease; pitfalls and promise. J Crohns Colitis 12 (Suppl 2): S641-S652, 2018.
65. Kvedaraite E, Lourda M, Ideström M, Chen P, Olsson-Åkefeldt S, Forkel M, Gavhed D, Lindforss U, Mjösberg J, Henter JI and Svensson M: Tissue-infiltrating neutrophils represent the main source of IL-23 in the colon of patients with IBD. Gut 65: 1632-1641, 2016.
66. Habas K and Shang L: Alterations in intercellular adhesion molecule 1 (ICAM-1) and vascular cell adhesion molecule 1 (VCAM-1) in human endothelial cells. Tissue Cell 54: 139-143, 2018.
67. Weber CR, Nalle SC, Tretiakova M, Rubin DT and Turner JR: Claudin-1 and claudin-2 expression is elevated in inflammatory bowel disease and may contribute to early neoplastic transformation. Lab Invest 88: 1110-1120, 2008.
68. Zhou J, Yu Y, Yang X, Wang Y, Song Y, Wang Q, Chen Z, Zong S, Fan M, Meng X, et al: Berberine attenuates arthritis in adjuvant-induced arthritic rats associated with regulating polarization of macrophages through AMPK/NF-κB pathway. Eur J Pharmacol 852: 179-188, 2019.
69. Li H, Li XL, Zhang M, Xu H, Wang CC, Wang S and Duan RS: Berberine ameliorates experimental autoimmune neuritis by suppressing both cellular and humoral immunity. Scand J Immunol 79: 12-19, 2014.

70. Wang Q, Qi J, Hu R, Chen Y, Kijlstra A and Yang P: Effect of berberine on proinflammatory cytokine production by ARPE-19 cells following stimulation with tumor necrosis factor-α. Invest Ophthalmol Vis Sci 53: 2395-2402, 2012.
71. Boulangé CL, Neves AL, Chilloux J, Nicholson JK and Dumas ME: Impact of the gut microbiota on inflammation, obesity, and metabolic disease. Genome Med 8: 42, 2008.
72. Ali L, Schnitzler JG and Kroon J: Metabolism: The road to inflammation and atherosclerosis. Curr Opin Lipidol 29: 474-480, 2018.
73. Xu F, Yang J, Meng B, Zheng JW, Liao Q, Chen JP and Chen XW: The effect of berberine on ameliorating chronic inflammatory pain and depression. Zhonghua Yi Xue Za Zhi 98: 1103-1108, 2018 (In Chinese).
74. Da Silva MS, Bigo C, Barbier O and Rudkowska I: Whey protein hydrolysate and branched-chain amino acids downregulate inflammation-related genes in vascular endothelial cells. Nutr Res 38: 43-51, 2017.
75. Chen YX, Gao QY, Zou TH, Wang BM, Liu SD, Sheng JQ, Ren JL, Zou XP, Liu ZJ, Song YY, *et al*: Berberine versus placebo for the prevention of recurrence of colorectal adenoma: A multicentre, double-blinded, randomised controlled study. Lancet Gastroenterol Hepatol 5: 267-275, 2020.